# Multibiometric Complex Fusion for Visible and Thermal Face Images

Ning Wang[1], Qiong Li[1*], Ahmed A. Abd El-Latif [1,2], Jialiang Peng[1, 3] and Xiamu Niu[1]

[1]*Harbin Institute of Technology, Harbin, 150080, China*
[2]*Menoufia University, Shebin El-Koom, 32511, Egypt*
[3]*Heilongjiang University, Harbin 150080, China*

*wangningtop@163.com, ahmed_rahiem@yahoo.com,peng80929@163.com and xiamu.niu@hit.edu.cn*

***Abstract***

*Unimodal biometric systems have to contend with various inherent limitations, such as restricted degrees of freedom, non-universality, susceptibility to spoofing attacks and unacceptable error rates. Multibiometric systems, which fuse two or more biometrics traits together, are able to effectively overcome most of these problems. In this paper, different face traits are fused considering convenient acquiring of visible face and the intrinsic anti-spoofing of thermal face. Initially, the complex fusion strategies at both pixel level and feature level are proposed, which can provide higher discrimination superiority. The 2D-classification methods, including 2DPCA, 2DLDA, $(2D)^2$PCA, $(2D)^2$LDA and $(2D)^2$FPCA are applied into the complex fusion, which can overcome the small size sample problems. Both identification and verification experiments are conducted on the NVIE visible and thermal face database. Various tests based on this database ascertain the efficacy of the proposed approaches in identification and verification. The better performances are in favor of the proposed approaches, FC_$(2D)^2$LDA and FC_$(2D)^2$FPCA, the training number 6 and 8, and the visible face fusion weight 0.4 and 0.6.*

***Keywords:*** *Multibiometric, Complex fusion, Visible and thermal face, Pixel level fusion, Feature level fusion, 2D-classification*

## 1. Introduction

With the rapid development of the world society, the need for reliable user authentication techniques has increased in the wake of heightened concerns about security and rapid advancements in networking, communication and mobility. Establishing the identification based on biometric systems has drawn much more attention recent decades [1]. Researchers have started to work on different kinds of biometric model, such as visible face [2], voice [3], thermal face [4], fingerprint [5], iris [6], vein [7], plamprint [8], lip [9], ear [10], *etc*. However, unimodel biometric system has to contend with inherent limitations such as noisy sensor data, large intra-class variations, restricted degrees of freedom, non-universality and unacceptable error rates. Another significant point is susceptibility to spoofing attacks [11-14]. Multibiometrics has attracted more interesting recently [15-17], because of addressing most of the above disadvantages effectively. Based on this, many large scale identification

* Corresponding author: qiong.li@hit.edu.cn

multibiometric systems have been widely adopted (*e.g.*, FBI's IAFIS, the Department of Homeland Security's US-VISIT, and the Government of India's UID) [18, 19].

The selection of attributes type should be considered deliberately. Visible and thermal face biometrics have been adopted into application. However, visible face imagery is sensitive to uncontrolled illumination conditions but is convenient. Thermal face imagery is affected by temperature changes but immune to forgery [20, 21]. Considering the acquiring convenience and application security, the fusion of visual and thermal face imagery is implemented to improve the performance of identification. Because of the inherent correlations of visible and thermal face and the solitary biometric traits [15, 22], we select pixel level and feature level fusion in this paper.

Numerous research efforts have been made on the fusion of visible and thermal face imagery during the last decade. Considering the homologous property of visible and thermal face imagery, several fusion algorithms based on multi-scale analysis (*e.g.*, DWT) are developed [23-26]. Neural network-based algorithms try to train useable parameters in transformed domain for robust multibiometric recognition [27-29]. Other researchers performed some effective methods to find an optimal strategy to perform multibiometrics, such as Genetic Algorithm (GA) [30, 31], Particle swarm optimization (PSO) [32], and so on [33-35]. Some contributions relay on PCA, LDA and KPCA [23, 24, 30]. All the above works show the competitive recognition performance. However, pixel level fusion in DWT domain has too much data to deal with. The neural network and optimization algorithms are time consuming. Besides, all these fusion approaches are based on the weight sum rule fusion sketch, which limits the advantages of discrimination of solitary sample. On the other side,, traditional PCA and LDA have small sample problems [36].

Yang *et al.*, [37] developed 2DPCA for image representation, which is based on 2D matrices rather than 1D vectors. It is easier to evaluate the covariance matrix accurately and less time is required to determine the corresponding eigenvectors [38]. Other 2D-based methods such as 2DLDA [39], $(2D)^2$PCA [40], $(2D)^2$LDA [41] and $(2D)^2$FPCA [42] also have the above superiorities. Yang *et al.*, [43] proposed the complex fisher method for face recognition to fuse face features. Wang *et al.*, [44] extend this complex method for multibiometrics based on KFDA. This method reflects the differences inherited from separately sensors comparing with weighted sum rule fusion strategy.

In this paper, we propose complex fusion approaches in pixel and feature level. At pixel level complex fusion, our strategy is to combine visible and thermal face imagery via complex vectors, and then to input them into an operation container called complex 2D-based methods (generated from 2DPCA, 2DLDA, $(2D)^2$PCA, $(2D)^2$LDA and $(2D)^2$FPCA) for a second feature extraction. At feature level complex fusion, we implement an alternative strategy to combine the 2D-based visible and thermal face features into a complex vector. Based on all the experimental comparisons, we give the selection suggestions of methodologies and parameters on NVIE visible and thermal face database.

The rest of this paper is organized as follows. Detailed of the proposed complex fusion approaches are given in Section 2. The experimental results and comparisons are discussed in Section 3. Finally, Section 4 concludes this paper.

## 2. Proposed Complex Fusion Approaches

### 2.1. 2D-based Complex Fusion in Pixel Level

In this section, we introduce the proposed complex fusion method of pixel level. The framework is shown in Figure 1. The visible and thermal face images are fused as different components of a complex vector, and then the features are extracted based on complex features using 2D-based methods.

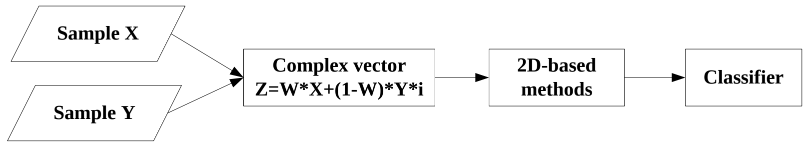


**Figure 1. The Illustration of Proposed Pixel Level Complex Fusion Strategy**

Suppose $Y$ and $Z$ are two image spaces defined on the pattern sample space $\Omega_p$. Given an arbitrary sample $x \in \Omega_p$, suppose the corresponding two images are $y \in Y$ and $z \in Z$ with same dimension. Our idea is to combine them into a complex vector via Eq. (1):

$$x = \omega \times y + (1-\omega) \times z \times i \tag{1}$$

where $\omega$ stands for the weight parameter, and $i$ is the imaginary unit.

Let $C^d$ be the combined sub-space on $\Omega_p$ expressed in Eq. (2), and the inner product for $C^d \subset \Omega_p$ can be defined as Eq. (3):

$$C^d = \{w \times y + (1-w) \times z \times i \mid y \in Y, z \in Z, w \in R\} \tag{2}$$

$$<\alpha, \beta> = \alpha^{\mathrm{H}} \beta, \forall \alpha, \beta \in C^d \tag{3}$$

where $H$ is the denotation of conjugate transpose. Under this inner product, we can easily prove that Eq. (3) satisfies:

- $<\alpha, \beta> = \overline{<\beta, \alpha>}$
- $<\alpha, \alpha> \geq 0$, where $<\alpha, \alpha> = 0$ if and only if $\alpha = 0$
- $<k_1\alpha_1 + k_2\alpha_2, \beta> = k_1 <\alpha_1, \beta> + k_2 <\alpha_2, \beta>, \forall \alpha_1, \alpha_2, \beta \in C^d, \forall k_1, k_2 \in R$

The space $C^d$ defined by the above inner product is a Unitary space. Let the training set be composed of $C$ classes, where each class contains $N$ samples, then we have the complex within-class scatter matrix, complex between-class scatter matrix and the complex total scatter matrix as given in Eqs. (4), (5) and (6).

$$S_w = \sum_{i=1}^{C} p(\omega_i) E\{(x - \overline{x}_i)(x - \overline{x}_i)^{\mathrm{H}} \mid \omega_i\} \tag{4}$$

$$S_b = \sum_{i=1}^{C} p(\omega_i)(\overline{x}_i - \overline{x})(\overline{x}_i - \overline{x})^{\mathrm{H}} \tag{5}$$

$$S_t = S_w + S_b = E\{(x - \overline{x})(x - \overline{x})^{\mathrm{H}}\} \tag{6}$$

where, $p(\omega_i)$ denotes the prior probability of $x$ belongs to class $i$, $\overline{x}_i$ and $\overline{x}$ denote the $i$ th sample mean and total sample mean, $E\{\cdot\}$ denotes the expectation operation. Usually,

$p(\omega_i) = 1/C$ . Eqs. (4), (5) and (6) are all semi-positive definite Hermite matrices [36]. Moreover, $S_w$ and $S_t$ are both positive definite matrix when $S_w$ is nonsingular [43].

In the light of the above, the complex 2DPCA criterion function can be defined as Eq. (7):

$$J(\phi) = \phi^{\mathrm{H}} G_t \phi \tag{7}$$

where $\phi$ is an $n$-dimensional nonzero vector, and $G_t$ is the image complex covariance matrix [37]. The 2DLDA criterion function is defined as Eq. (8):

$$J(\phi) = \frac{\phi^{\mathrm{H}} G_b \phi}{\phi^{\mathrm{H}} G_w \phi} \tag{8}$$

where $G_b$ is the image complex between-class scatter matrix and $G_w$ the image complex within-class scatter matrix [39].

Since $S_w$ is positive definite and $S_b$ is semi-positive definite, for any arbitrary $\phi$ , we have $\phi^{\mathrm{H}} G_t \phi \geq 0$ , $\phi^{\mathrm{H}} G_b \phi \geq 0$ and $\phi^{\mathrm{H}} G_w \phi > 0$ . This means that the values of $J(\phi)$ are all nonnegative. So, the physical meaning of the complex 2D-based discrimination criterion defined in Unitary space is similar to the classical 2D-based discrimination criterion defined in Euclidean space.

The vector $\phi^*$ maximizing the complex total scatter is called complex 2D-based optimal projection direction. The physical meaning is that after the projection of samples onto $\phi^*$, the square error sum of complex image samples is minimized in Unitary space. However, the single optimal projection direction is generally not enough in real-world applications. The direction of $\phi$ is more important than its amplitude. We could get the optimal projection axis which are the eigenvectors of $G_t$ for 2DPCA and of $G_w^{-1} G_b$ for 2DLDA corresponding to the several largest eigenvalues.

The feature extraction method described above is called pixel level complex 2D-based method denoted as PC_2DPCA and PC_2DLDA. On the same principle, we can get the discrimination criterion function of $(2D)^2$PCA, (2D)2LDA and $(2D)^2$FPCA. Obviously, the traditional 2D-based methods are the special case of complex 2D-based methods. Generally, we can extend this pixel level complex fusion methodology to these 2D-based approaches.

### 2.2. 2D-Based Complex Fusion in Feature Level

This section gives the simply description of complex feature level fusion. It is clearly that Figure 2 shows its framework. Visible and thermal face imageries features are extracted using 2D-based methods, and are fused into a complex vector as different components.

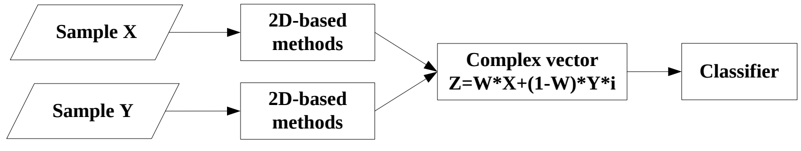


**Figure 2. The Illustration of Proposed Feature Level Complex Fusion Strategy**

Suppose $Y_f$ and $Z_f$ are two feature spaces defined on the 2D-based feature space $\Omega_f$. Given an arbitrary feature vector $x_f \in \Omega_f$, suppose the corresponding two 2D-based features are $y_f \in Y_f$ and $z_f \in Z_f$ with the same dimension. The idea is to combine them via Eq. (9):

$$x_f = w \times y_f + (1-w) \times z_f \times i \tag{9}$$

Note that, if the dimensions of $y_f$ and $z_f$ are not equal, then padding the lower dimensional one with zeros until its dimension is equal to the others' before combination. Obviously, the space $\Omega_f$ is an $n$ dimensional complex vector space, where $n = max\{dimY_F, dimZ_F\}$. The features $y_f$ and $z_f$ can be extracted by any feature extraction method. Our aim is to propose 2D-based method for feature extraction implementation.

### 2.3. Complex Feature Vector Distance

In our fusion system, each class has the respective feature complex template matrix $\hat{D}_T (T = 1,...,C)$. During recognition, let $\hat{D}_{test}$ be a given complex image for recognition, then the $\|.\|_2$ between $\hat{D}_{test}$ and the template $\hat{D}_T$ based nearest neighbor classifier is used for classification. The distance $Dis$ between $\hat{D}_{test}$ and $\hat{D}_T$ can be defined as Eq. (10):

$$Dis(\hat{D}_{test}, \hat{D}_T) = \| \hat{D}_{test} - \hat{D}_T \|_2 = \sqrt{(\hat{D}_{test} - \hat{D}_T)^{\mathrm{H}} (\hat{D}_{test} - \hat{D}_T)} \tag{10}$$

## 3. Performance Evaluation with Multi-Modal Biometrics

In this section, results of multi-model matching experiments are presented. Several existing thermal and visible face fusion algorithms and proposed complex fusion algorithms are conducted on a visible and thermal face database. Several evaluation protocols including EER, ROC cuve, and recognition rate are carried out for the algorithm performance.

False Reject Rate (FRR) and False Accept Rate (FAR) are used to test the performance of the whole recognition system. However, False Matching Rate (FMR) and False Non-Matching Rate (FNMR) are preferred to evaluate the performance of the algorithms in an off-line technology test [45]. ROC curve is a plot of FMR(t) against 1-FNMR(t) for various decision thresholds *t*, and provides more direct view of the error-vs-error tradeoff. The Equal Error Rate (EER, when FMR=FNMR) can be acquired from the performance curves. For every evaluation index, the heat maps are also provided to indicate which parameters are better for performance. The larger the value, the more warm the colors, and vice versa.

### 3.1. Database Description

Proposed algorithm for thermal face image is tested on the Natural Visible and Infrared facial Expression (termed NVIE) database which is constructed by The Key Laboratory of Computing and Communication Software of Anhui Province (CCSL). It contains six different expressions as shown in Figure 3, and is recorded simultaneously by a visible and an infrared thermal camera. The posed database also includes expression image sequences with and without glasses [46]. We utilize the sub-database including 90 classes, which contains 12 samples with six expressions, to test the proposed approaches and the other existing methods.

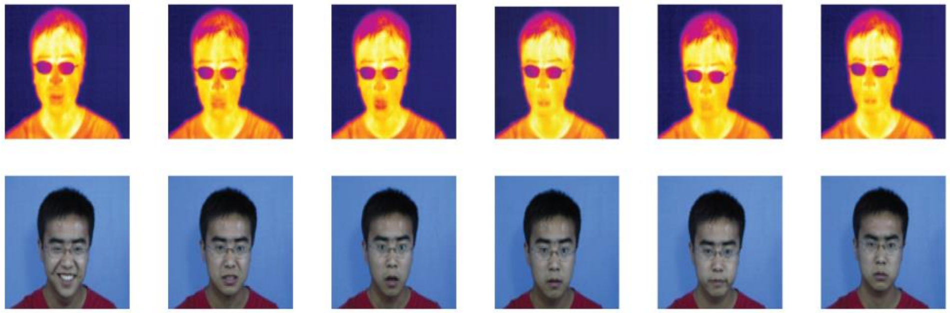

**Figure 3. The Samples in NVIE Thermal Database**

### 3.2. Comparison between proposed PC_2DPCA and the other Fusion Approaches

The recognition comparisons between the proposed complex fusion strategy PC_2DPCA, and other approaches can be seen in Table 1. The configurations of every method are explained in the following:

- PF_PCA: Fuse in pixel level and then use PCA [23].
- DF_PCA: Fuse the coefficients of DWT and then implement iDWT and PCA [24].
- PCA_GA: Get PCA feature, and then use GA to find a better fusion strategy [31].
- PCA_KNN: Get PCA feature for fusion, and then use KNN for matching [34].
- DP_MLP: Get DWT PCA feature for fusion, then use Multi-layer percept neural net[27].
- PCA_PSO: Get PCA feature, and then use PSO to find a better fusion strategy [32].
- IPCA_SVM: Get IPCA feature for fusion, and then use SVM for matching [35].
- PC_2DPCA: Proposed PC_2DPCA for feature extraction in pixel level fusion.

**Table 1. The Comparison of Different Approaches for NVIE Database**

| Method | Recognition rate(%) |
|---|---|
| PF_PCA [23] | 89.53 |
| DF_PCA [24] | 89.53 |
| PCA_GA [31] | 93.31 |
| PCA_KNN [34] | 89.37 |
| DP_MLP [27] | 92.51 |
| PCA_PSO [32] | 91.26 |
| IPCA_SVM [35] | 90.72 |
| PC_2DPCApro | 94.02 |

These experiments are performed in 5 training and 7 testing samples. From Table 1, we can find out that, there is no difference in methods PF_PCA and DF_PCA. Though methods DP_MLP, PCA_GAs and PCA_PSO give a little better recognition performance, the operation is time-consuming. The iteration of DF_MLP in our experiment is 11000, and it takes more than one hour for running. The generations of PCA_GA and PCA_PSO are 100, and the population is 80. Method IPCA_SVM and PCA_KNN haven't played the best performance as we expected either. The proposed pixel level complex fusion method

PC_2DPCA shows the best result. That's because PC_2DPCA not only extract feature in two dimensional, the more important reason is it puts every feature into different matching space separately.

### 3.3. Performance Comparisons between Proposed Approaches

**3.3.1. Experiment Setup:** In the following experiments, we test the performance of proposed pixel level complex (PC) and feature level complex (FC) fusion algorithms. To compare the different approaches in detail, we conduct the following experiments in diverse training number $trn$ and visible face fusion weight $\omega$. We fix the total number of samples to 12 for every class in the NVIE database. Those $trn$ images are randomly selected from each class to construct the training data set, and the remaining images are used for testing. To ensure sufficient training and simplify article, the training number of $trn$ starts from at least 2 and at intervals of 2, and the visible face fusion weight $\omega$ starts from at least 0.2 and at intervals of 0.2.

**Table 2. The Abbreviations of Different Methods**

| NO. | Abbrev. | Description |
|---|---|---|
| 1 | M1 | 2DPCA |
| 2 | M2 | 2DLDA |
| 3 | M3 | $(2D)^2$PCA |
| 4 | M4 | $(2D)^2$LDA |
| 5 | M5 | $(2D)^2$FPCA |

In order to specifically measure the effectiveness of proposed approach, different abbreviations of the proposed and conventional methods are compared. The abbreviation of each method is illustrated in Table 2.

**3.3.2. Verification Performance of Pixel Level and Feature Level Complex Fusion Strategies:** This section compares the verification performance of different approaches. Table 3 and Table 4 show the EER of different approaches in different parameters. The best EER of every method is shown in under line, and the worst EER is shown in under wave line. The better EERs in PC fusion methods distribute in larger training numbers 6, 8 and 10. And in FC fusion methods, they distribute in training number 10 mainly.

**Table 3. EER of Pixel-based Complex Algorithms**

| No. | $(trn, \omega)$ | Pixel-based complex algorithms | | | | |
|---|---|---|---|---|---|---|
| | | PC_M1 | PC_M2 | PC_M3 | PC_M4 | PC_M5 |
| 1 | (2, 0.2) | 0.1498 | 0.1263 | 0.1471 | 0.1348 | 0.1297 |
| 2 | (2, 0.4) | 0.0976 | 0.0923 | 0.0987 | 0.0895 | 0.0850 |
| 3 | (2, 0.6) | 0.0763 | 0.0854 | 0.0793 | 0.0913 | 0.0736 |
| 4 | (2, 0.8) | 0.0907 | 0.1050 | 0.0920 | 0.1018 | 0.0894 |
| 5 | (4, 0.2) | 0.1251 | 0.1036 | 0.1240 | 0.1068 | 0.0912 |
| 6 | (4, 0.4) | 0.0791 | 0.0721 | 0.0792 | 0.0626 | 0.0519 |
| 7 | (4, 0.6) | 0.0573 | 0.0676 | 0.0601 | 0.0633 | 0.0435 |
| 8 | (4, 0.8) | 0.0840 | 0.0914 | 0.0860 | 0.0800 | 0.0652 |
| 9 | (6, 0.2) | 0.1088 | 0.0918 | 0.1084 | 0.0884 | 0.0737 |

| | | | | | | |
|---|---|---|---|---|---|---|
| 10 | (6, 0.4) | 0.0693 | 0.0620 | 0.0674 | 0.0464 | 0.0405 |
| 11 | (6, 0.6) | **0.0473** | 0.0454 | **0.0475** | 0.0501 | 0.0387 |
| 12 | (6, 0.8) | 0.0589 | 0.0699 | 0.0626 | 0.0577 | 0.0490 |
| 13 | (8, 0.2) | 0.1003 | 0.0766 | 0.0980 | 0.0679 | 0.0522 |
| 14 | (8, 0.4) | 0.0527 | 0.0423 | 0.0559 | **0.0350** | 0.0302 |
| 15 | (8, 0.6) | 0.0486 | **0.0413** | 0.0496 | 0.0371 | 0.0384 |
| 16 | (8, 0.8) | 0.0566 | 0.0664 | 0.0599 | 0.0491 | 0.0474 |
| 17 | (10, 0.2) | 0.1003 | 0.0711 | 0.0891 | 0.0653 | 0.0609 |
| 18 | (10, 0.4) | 0.0619 | 0.0455 | 0.0593 | 0.0415 | **0.0278** |
| 19 | (10, 0.6) | 0.0603 | 0.0483 | 0.0600 | 0.0421 | 0.0417 |
| 20 | (10, 0.8) | 0.0739 | 0.0680 | 0.0732 | 0.0637 | 0.0402 |

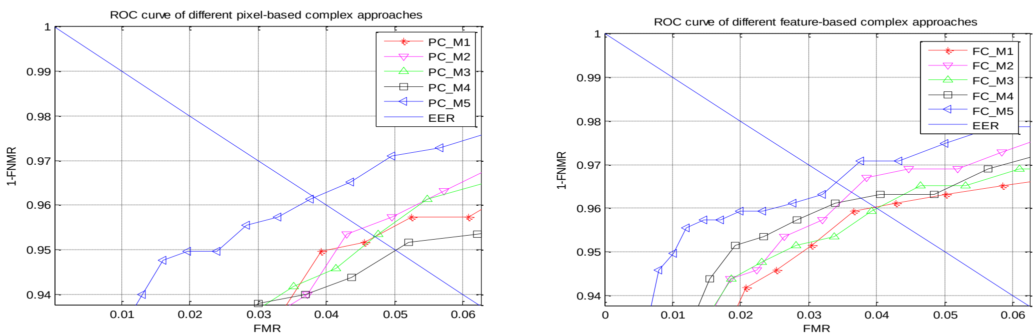


(a) ROC curve of PC methods (b) ROC curve of FC methods

**Figure 4. The recognition Performance of Different Complex Methods**

To compare the recognition performance of different complex approaches, Figure 4 shows the recognition results in parameter (6, 0.6). Obviously, method PC_M5 gives the best performance among pixel level complex approaches in Figure 4(a). Comparing Figure 4(a) and Figure 4(b), the results of feature-based complex approaches are better and more concentrated than the results of pixel-based complex approaches. From heat maps in Figure 5(a) and Figure 5(b), we can see that the better parameters are concentrated in the lower right part of heat maps. It means the performance turns better as the training number increases. Figure 6 illustrates this phenomenon deeply, which shows the EER of PC and FC fusion approaches in all the parameters. Figure 6(a) and Figure 6(b) also illustrate that the visible face fusion weight ω is better in 0.4 and 0.6, and is a little worse in 0.2 or 0.8. It means that the ratio of visible and thermal face should not be too large.

**Table 4. EER of Feature-Based Complex Algorithms**

| No. | $(trn, \omega)$ | Feature-based complex algorithms | | | | |
|---|---|---|---|---|---|---|
| | | FC_M1 | FC_M2 | FC_M3 | FC_M4 | FC_M5 |
| 1 | (2, 0.2) | 0.1149 | 0.1080 | 0.1108 | 0.1197 | 0.1191 |
| 2 | (2, 0.4) | 0.0787 | 0.0719 | 0.0744 | 0.0823 | 0.0739 |
| 3 | (2, 0.6) | 0.0726 | 0.0862 | 0.0693 | 0.0943 | 0.0736 |
| 4 | (2, 0.8) | 0.0940 | 0.1035 | 0.0944 | 0.1044 | 0.0900 |
| 5 | (4, 0.2) | 0.0987 | 0.0802 | 0.0953 | 0.0831 | 0.0805 |
| 6 | (4, 0.4) | 0.0654 | 0.0566 | 0.0585 | 0.0546 | 0.0494 |
| 7 | (4, 0.6) | 0.0552 | 0.0563 | 0.0569 | 0.0532 | 0.0482 |

| | | | | | | |
|---|---|---|---|---|---|---|
| 8 | (4, 0.8) | 0.0789 | 0.0751 | 0.0762 | 0.0731 | 0.0629 |
| 9 | (6, 0.2) | 0.0907 | 0.0735 | 0.0846 | 0.0781 | 0.0678 |
| 10 | (6, 0.4) | 0.0524 | 0.0467 | 0.0490 | 0.0380 | 0.0441 |
| 11 | (6, 0.6) | 0.0398 | 0.0365 | 0.0403 | 0.0375 | 0.0339 |
| 12 | (6, 0.8) | 0.0559 | 0.0582 | 0.0576 | 0.0560 | 0.0446 |
| 13 | (8, 0.2) | 0.0781 | 0.0649 | 0.0727 | 0.0552 | 0.0557 |
| 14 | (8, 0.4) | 0.0340 | 0.0302 | 0.0335 | **0.0245** | 0.0249 |
| 15 | (8, 0.6) | 0.0385 | 0.0307 | 0.0367 | 0.0307 | 0.0267 |
| 16 | (8, 0.8) | 0.0578 | 0.0523 | 0.0586 | 0.0421 | 0.0433 |
| 17 | (10, 0.2) | 0.0776 | 0.0601 | 0.0696 | 0.0503 | 0.0527 |
| 18 | (10, 0.4) | **0.0305** | **0.0302** | **0.0296** | 0.0256 | **0.0241** |
| 19 | (10, 0.6) | 0.0350 | 0.0378 | 0.0340 | 0.0344 | 0.0361 |
| 20 | (10, 0.8) | 0.0661 | 0.0650 | 0.0673 | 0.0465 | 0.0360 |

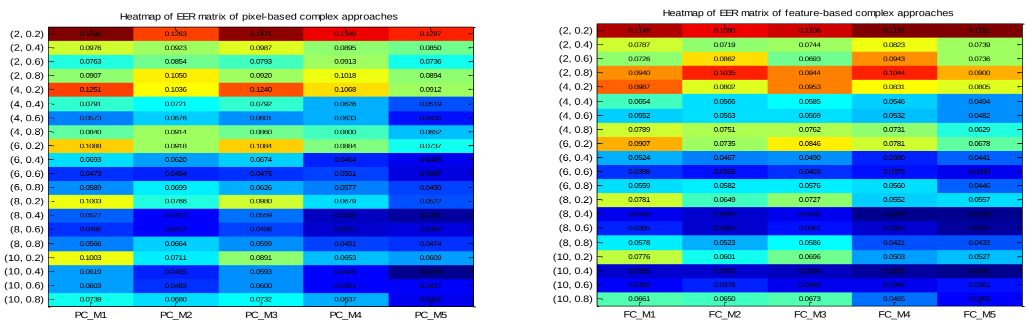


(a) Heat map of EER of PC methods (b) Heat map of EER of FC methods

**Figure 5. The Heat Maps of EER Matrixes of Different Complex Methods**

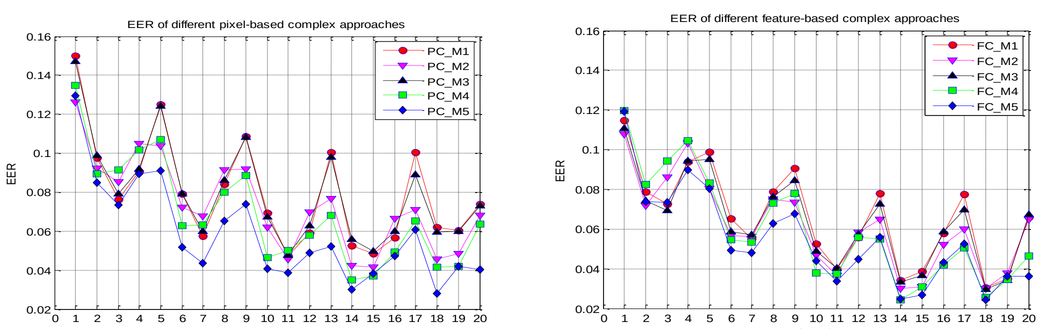


(a) EER of PC algorithms (b) EER of FC algorithms

**Figure 6. The EER of Different Complex Methods**

**3.3.3. Identification Performance of PC and FC Approaches:** The identification performance comparisons of different approaches in feature level are discussed in this section. Table 5 and Table 6 show the recognition rates of different approaches in different parameters. The best results of every method are also shown in under line, and the worst results are shown in under wave line. The best rates in PC and FC fusion methods also distribute in larger training numbers. The heat maps of rate matrixes are shown in Figure 7. From Figure 7(a) and

Figure 7(b), the better parameters are also concentrated in the lower right part of heat maps. Figure 8 shows the same phenomenon as Figure 6 shows.

Pixel-based complex fusion approaches implement scatter matrix computing operation in complex matrix directly, this takes too much data and makes the computing more complex. Feature-based complex fusion approaches compute scatter matrix first, and then fuse together. This kind of computing method only put less features into complex space and makes the matching more precise.

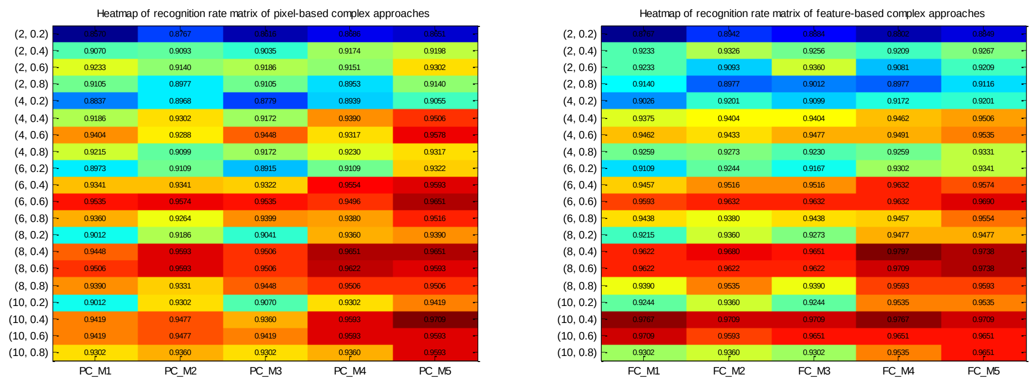


(a) Heat map of rate of PC methods (b) Heat map of matrix of FC methods

**Figure 7. The Heat Maps of Rate Matrixes of Different Complex Methods**

**Table 5. Recognition Rate of Pixel-based Complex Algorithms**

| No. | $(trn, \omega)$ | Pixel-based complex algorithms | | | | |
|---|---|---|---|---|---|---|
| | | PC_M1 | PC_M2 | PC_M3 | PC_M4 | PC_M5 |
| 1 | (2, 0.2) | 0.8570 | 0.8767 | 0.8616 | 0.8686 | 0.8651 |
| 2 | (2, 0.4) | 0.9070 | 0.9093 | 0.9035 | 0.9174 | 0.9198 |
| 3 | (2, 0.6) | 0.9233 | 0.9140 | 0.9186 | 0.9151 | 0.9302 |
| 4 | (2, 0.8) | 0.9105 | 0.8977 | 0.9105 | 0.8953 | 0.9140 |
| 5 | (4, 0.2) | 0.8837 | 0.8968 | 0.8779 | 0.8939 | 0.9055 |
| 6 | (4, 0.4) | 0.9186 | 0.9302 | 0.9172 | 0.9390 | 0.9506 |
| 7 | (4, 0.6) | 0.9404 | 0.9288 | 0.9448 | 0.9317 | 0.9578 |
| 8 | (4, 0.8) | 0.9215 | 0.9099 | 0.9172 | 0.9230 | 0.9317 |
| 9 | (6, 0.2) | 0.8973 | 0.9109 | 0.8915 | 0.9109 | 0.9322 |
| 10 | (6, 0.4) | 0.9341 | 0.9341 | 0.9322 | 0.9554 | 0.9593 |
| 11 | (6, 0.6) | **0.9535** | 0.9574 | **0.9535** | 0.9496 | 0.9651 |
| 12 | (6, 0.8) | 0.9360 | 0.9264 | 0.9399 | 0.9380 | 0.9516 |
| 13 | (8, 0.2) | 0.9012 | 0.9186 | 0.9041 | 0.9360 | 0.9390 |
| 14 | (8, 0.4) | 0.9448 | **0.9593** | 0.9506 | **0.9651** | 0.9651 |
| 15 | (8, 0.6) | 0.9506 | **0.9593** | 0.9506 | 0.9622 | 0.9593 |
| 16 | (8, 0.8) | 0.9390 | 0.9331 | 0.9448 | 0.9506 | 0.9506 |
| 17 | (10, 0.2) | 0.9012 | 0.9302 | 0.9070 | 0.9302 | 0.9419 |
| 18 | (10, 0.4) | 0.9419 | 0.9477 | 0.9360 | 0.9593 | **0.9709** |
| 19 | (10, 0.6) | 0.9419 | 0.9477 | 0.9419 | 0.9593 | 0.9593 |
| 20 | (10, 0.8) | 0.9302 | 0.9360 | 0.9302 | 0.9360 | 0.9593 |

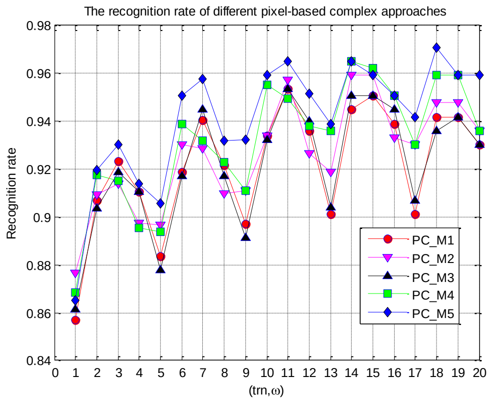


(a) Recognition rates of PC methods

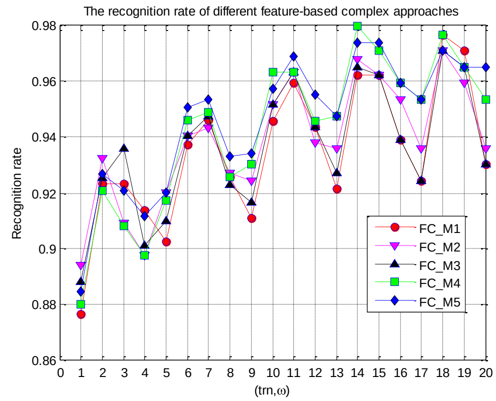


(b) Recognition rates of PC methods

**Figure 8. The Recognition Rate of Different complex methods**

**Table 6. Recognition Rate of Feature-based Complex Algorithms**

| No. | $(trn,\omega)$ | Feature-based complex algorithms | | | | |
|---|---|---|---|---|---|---|
| | | FC_M1 | FC_M2 | FC_M3 | FC_M4 | FC_M5 |
| 1 | (2, 0.2) | 0.8767 | 0.8942 | 0.8884 | 0.8802 | 0.8849 |
| 2 | (2, 0.4) | 0.9233 | 0.9326 | 0.9256 | 0.9209 | 0.9267 |
| 3 | (2, 0.6) | 0.9233 | 0.9093 | 0.9360 | 0.9081 | 0.9209 |
| 4 | (2, 0.8) | 0.9140 | 0.8977 | 0.9012 | 0.8977 | 0.9116 |
| 5 | (4, 0.2) | 0.9026 | 0.9201 | 0.9099 | 0.9172 | 0.9201 |
| 6 | (4, 0.4) | 0.9375 | 0.9404 | 0.9404 | 0.9462 | 0.9506 |
| 7 | (4, 0.6) | 0.9462 | 0.9433 | 0.9477 | 0.9491 | 0.9535 |
| 8 | (4, 0.8) | 0.9259 | 0.9273 | 0.9230 | 0.9259 | 0.9331 |
| 9 | (6, 0.2) | 0.9109 | 0.9244 | 0.9167 | 0.9302 | 0.9341 |
| 10 | (6, 0.4) | 0.9457 | 0.9516 | 0.9516 | 0.9632 | 0.9574 |
| 11 | (6, 0.6) | 0.9593 | 0.9632 | 0.9632 | 0.9632 | 0.9690 |
| 12 | (6, 0.8) | 0.9438 | 0.9380 | 0.9438 | 0.9457 | 0.9554 |
| 13 | (8, 0.2) | 0.9215 | 0.9360 | 0.9273 | 0.9477 | 0.9477 |
| 14 | (8, 0.4) | 0.9622 | 0.9680 | 0.9651 | **0.9797** | **0.9738** |
| 15 | (8, 0.6) | 0.9622 | 0.9622 | 0.9622 | 0.9709 | **0.9738** |
| 16 | (8, 0.8) | 0.9390 | 0.9535 | 0.9390 | 0.9593 | 0.9593 |
| 17 | (10, 0.2) | 0.9244 | 0.9360 | 0.9244 | 0.9535 | 0.9535 |
| 18 | (10, 0.4) | **0.9767** | **0.9709** | **0.9709** | 0.9767 | 0.9709 |
| 19 | (10, 0.6) | 0.9709 | 0.9593 | 0.9651 | 0.9651 | 0.9651 |
| 20 | (10, 0.8) | 0.9302 | 0.9360 | 0.9302 | 0.9535 | 0.9651 |

### 3.4. Remarks

In the light of the experimental results, the performances of feature level complex fusion approaches are better than the pixel level complex fusion ones. Based on comprehensive consideration of EER and recognition rate, we suggest the parameters could be selected in the middle right of corresponding parameter matrix. The best results are in favor of are

FC_$(2D)^2$LDA and FC $(2D)^2$FPCA. The appropriate training numbers are 6 and 8, and the visible face sample fusion weight are 0.4 and 0.6.

## 4. Conclusion

In biometric systems, unimodel biometric systems have inherent problems and multibiometric systems can address most of their limitations. Considering the acquiring convenience and application security, the fusion of visible and thermal face images is proposed in this paper. The proposed approaches deal with the problems of multibiometric fusion using 2D-based algorithms in pixel level and feature level. The theoretical derivation of pixel level complex fusion approach PC_2DPCA and PC_2DLDA are proposed, and also be extended to 2D-based classification methods: $(2D)^2$PCA, $(2D)^2$LDA and $(2D)^2$FPCA. Besides, the complex fusion methods in feature level for visible and thermal face images are proposed. These methods evaluate the covariance matrix accurately and reflect the differences inherited from separately sensors. All the approaches are tested in the multimodal database NVIE that contains visible and thermal face images with six different expressions. Several experiments conducted on this database ascertain the efficacy of the proposed approaches in identification and verification. In the light of the experimental tests, the best results are in favor of the proposed approaches, FC_$(2D)^2$LDA and FC_$(2D)^2$FPCA, the training number 6 and 8, and the visible face fusion weight 0.4 and 0.6.

## Acknowledgements

This work is supported by the Fundamental Research Funds for the Central Universities (Grant Number: HIT. NSRIF. 2013061).

## References

[1] A. K. Jain, P. Flynn and A. A. Ross, "Intrduction of Handbook of Biometrics", USA Springer Publisher, New York, **(2008)**, pp. 1-22.
[2] I. Naseem, R. Togneri and M. Bennamoun, "Linear Regression for Face Recognition", IEEE Trans. Pattern. Anal. Mach. Intell., vol. 32, no. 11, **(2010)**, pp. 1-6.
[3] B. Carrara and C. Adams, "You Are the Key: Generating Cryptographic Keys from Voice Biometrics", Proceedings of the 8th Annual International Conference on Privacy Security and Trust, Ottawa, Canada, **(2010)** August 17-19, pp. 213-222.
[4] N. Wang, Q. Li, J. Peng, A. A. A. El-Latif and X. Niu, "An Enhanced Thermal Face Verification Method Based on Multi-Scale Complex Fusion for Gabor Coefficients", Submitted to Multimed. Tools Appl., under consideration, **(2012)**, pp. 1-19.
[5] V. Conti, C. Militello, F. Sorbello and S. Vitabile, "Introducing Pseudo-singularity Points for Efficient Fingerprints Classification and Recognition", Proceedings of the 4th International Conference on Complex, Intelligent and Software Intensive Systems. Krakow, Poland, **(2010)** February 15-18, pp. 368-375.
[6] N. Wang, Q. Li, A. A. A. El-Latif, T. Zhang and X. Niu, "Toward Accurate Localization and High Recognition Performance for Noisy Iris Images", Multimed. Tools Appl., **(2012)**, pp. 1-20.
[7] G. Yang, X. Xi and YilongYin, "Finger Vein Recognition Based on A Personalized Best Bit Map", Sensors, vol. 12, no. 2, **(2012)**, pp. 1738-1757.
[8] R. Wang, D. Ramos and J. Fierrez, "Improving Radial Triangulation-Based Forensic Palmprint Recognition According to Point Pattern Comparison by Relaxation", Proceedings of the 5th IAPR International Conference on Biometrics, New Delhi, India, **(2012)** March 29- April 1, pp. 427-432.
[9] A. Sayo, Y. Kajikawa and M. Muneyasu, "Biometrics Authentication Method using Lip Motion in Utterance", Proceedings of the 8th International Conference on Information, Communications and Signal Processing, Singapore, Singapore, **(2011)** December 13-16, pp. 1-5.

[10] B. G. Kim, S. Y. Jung and D. J. Park, “Robust Profile Verification Scheme Based on Ear Reference Coordinate System”, Int. J. Pattern. Recogn., vol. 18, no. 4, **(2004)**, pp. 685-700.
[11] J. Feng and A. K. Jain, “Fingerprint Reconstruction: From Minutiae to Phase”, IEEE Trans. Pattern. Anal. Mach. Intell., vol. 33, no. 2, **(2011)**, pp. 209-223.
[12] J. Galbally, J. Fierrez, J. Ortega-Garcia, C. McCool and S. Marcel, “Hill-climbing Attack to An Eigenface-Based Face Verification System”, Proceedings of the 1st IEEE International Conference on Biometrics, Identity and Security, Tampa, FL, United states, **(2009)** September 22-23, pp. 1-6.
[13] G. Wang and H. Wu, “Research And Realization on Voice Restoration Technique for Voice Communication Software”, Proceedings of the International Symposium on Information Engineering and Electronic Commerce, Ternopil, Ukraine, **(2009)** May 16-17, pp. 791-795.
[14] S. Venugopalan and M. Savvides, “How to Generate Spoofed Irises from An Iris Code Template”, IEEE Trans. Inf. Foren. Sec., vol. 6, no. 2, **(2011)**, pp. 385-395.
[15] A. Ross and A. K. Jain, “Multimodal Biometrics: An Overview”, Proceedings of the 12th European Signal Processing Conference, **(2004)** August, pp. 1221-1224.
[16] V. M. Mane and D. V. Jadhav, “Review Of Multimodal Biometrics: Applications, Challenges and Research Areas”, Int. J. Biomet. Bioinf., vol. 3, no. 5, **(2009)**, pp. 90-95.
[17] B. J. Kang, K. R. Park, J. H. Yoo and J. N. Kim, “Multimodal Biometric Method That Combines Veins”, Prints and Shape of A Fnger, Opt. Eng., vol. 50, **(2011)**, pp. 1-13.
[18] 3m cogent, http:www.cogentsystems.com/fusiond3asp.
[19] A multi-biometric matching architecture [online]. http:www.morphotrak.com/MorphoTrak /MorphoTrak/mtmulti-biometrics.html.
[20] D. Socolinsky and A. Selinger, “Thermal Face Recognition over Time”, Proceedings of the 17th International Conference on Pattern Recognition, **(2004)** Auguest 23-26, pp. 187-190.
[21] G. Hermosilla, J. del Solar, R. Verschae and M. Correa, “A Comparative Study of Thermal Face Recognition Methods in Unconstrained Environments”, Pattern. Recogn., vol. 45, no. 7, **(2012)**, pp. 2445-2459.
[22] A. K. Jain and A. Ross, “Multibiometric Systems”, Commun. ACM., vol. 47, no. 1, **(2004)**, pp. 34-40.
[23] B. Abidi, S. Huq and M. Abidi, “Fusion of Visual, Thermal and Range as A Solution to Illumination and Pose Restrictions in Face Recognition”, Proceedings of the IEEE 38th Annual 2004 International Carnahan Conference on Security Technology, Albuquerque, NM, United states, **(2004)** October 11-14, pp. 325-330.
[24] O. K. Kwon and S. G. Kong, “Multiscale Fusion of Visual and Thermal Images for Robust Face Recognition”, Proceedings of the IEEE Intemational Conference on Computational Intelligence for Homeland Security and Personal Safety, Orlando, FL, United states, **(2005)** March 31-April 1, pp. 112-116.
[25] S. Moon, S. G. Kong, J. H. Yoo and K. Chung, “Face Recognition With Multiscale Data Fusion of Visible and Thermal Images”, Proceedings of the IEEE International Conference on Computational Intelligence for Homeland Security and Personal Safety, Alexandria, VA, United states, **(2006)** October 16-17, pp. 24-27.
[26] S. G. Kong, J. Heo, F. Boughorbel, Y. Zheng, B. R. Abidi, A. Koschan, M. Yi and M. A. Abidi, “Multiscale Fusion of Visible and Thermal IR Images for Illumination-Invariant Face Recognition”, Int. J. Comput. Vision., vol. 71, no. 2, **(2007)**, pp. 215-233.
[27] M. K. Bhowmik, D. Bhattacharjee, M. Nasipuri and Dipak, “Optimum Fusion of Visual and Thermal Face Images for Recognition”, Proceedings of the 6th International Conference on Information Assurance and Security, Atlanta, GA, United states, **(2010)** August 23-25, pp. 311-316.
[28] M. K. Bhowmik, D. Bhattacharjee, M. Nasipuri, D. K. Basu and M. Kundu, “Fusion of Wavelet Coefficients From Visual and Thermal Face Images for Human Face Recognition-A Comparative Study”, J. Image. Proc., vol. 4, no. 1, **(2010)**, pp. 1-12.
[29] M. K. Bhowmik, D. Bhattacharjee, D. K. Basu and M. Nasipuri, “Polar Fusion Technique Analysis for Evaluating The Performances of Image Fusion of Thermal and Visual Images for Human Face Recognition”, Proceedings of the IEEE Workshop on Computational Intelligence in Biometrics and Identity Management, Paris, France, **(2011)** April 11-15, pp.62-69.
[30] G. Bebis, A. Gyaourova, S. Singh and I. Pavlidis, “Face Recognition by Fusing Thermal Infrared and Visible Imagery”, Image. Vision. Comput., vol. 24, no. 7, **(2006)**, pp. 727-742.
[31] M. Shahbe and S. Hati, “IR and Visible Face Recognition Using Fusion of Kernel Based Features”, Proceedings of the 19th International Conference on Pattern Recognition, Tampa, FL, United states, **(2008)** December 8-11, pp. 1-4.
[32] R. Raghavendra, BernadetteDorizzi, A. Rao and G.HemanthaKumar, “Particle Swarm Optimization Based Fusion of Near Infrared and Visible Images for Improved Face Verification”, Pattern. Recogn., vol. 44, no. 2, **(2011)**, pp. 401-411.
[33] R. Singh, M. Vatsa and A. Noore, “Integrated Multilevel Image Fusion and Match Score Fusion of Visible and Infrared Face Images for Robust Face Recognition”, Pattern. Recogn., vol. 41, no. 2, **(2008)**, pp. 880-893.

[34] F. M. Pop, M. Gordan, C. Florea and A. Vlaicu, "Fusion Based Approach for Thermal and Visible Face Recognition Under Pose and Expressivity Variation", Proceedings of the 9th RoEduNet IEEE International Conference, Sibiu, Romania, **(2010)** June 24-26, pp. 311-316.
[35] M. K. Bhowmik, B. K. De, D. Bhattacharjee, D. K. Basu and M. Nasipuri, "Multisensor Fusion of Visual and Thermal Images for Human Face Identification Using Different SVM Kernels", Proceedings of the IEEE Long Island Systems, Applications and Technology Conference, Farmingdale, NY, **(2012)** May 4, pp. 1-7.
[36] J. Yang, J. yu Yang, D. Zhang and J. feng Lu, "Feature Fusion: Parallel Strategy VS. Serial Strategy", Pattern. Recogn., vol. 36, no. 6, **(2003)**, pp. 1369-1381.
[37] J. Yang, D. Zhang, A. F. Frangi and J. yu Yang, "Two-Dimensional PCA: A New Approach to Appearance-Based Face Representation and Recognition", IEEE Trans. Pattern. Anal. Mach. Intell., vol. 26, no. 1, **(2004)**, pp. 131-137.
[38] Y. G. Kima, Y. J. Songa, U. D. Changa, D. W. Kimb, T. S. Yunc and J. H. Ahna, "Face Recognition Using A Fusion Method Based on Bidirectional 2DPCA", Appl. Math. Comput., vol. 25, no. 2, **(2008)**, pp. 601-607.
[39] M. Li and B. Yuan, "2DLDA: A Statistical Linear Discriminant Analysis for Image Matrix", Pattern Recognit. Lett., vol. 26, no. 5, **(2005)**, pp. 527-532.
[40] D. Zhang and Z. H. Zhou, "$(2D)^2$PCA: Two-Directional Two-Dimensional PCA for Efficient Face Representation and Recognition", Neurocomputing, vol. 69, no. 1-3, **(2005)**, pp. 224-231.
[41] S. Noushath, G. H. Kumar and P. Shivakumara, "$(2D)^2$LDA: An Efficient Approach for Face Recognition", Pattern Recognit., vol. 39, no. 7, **(2006)**, pp. 1396-1400.
[42] C. Yu, H. Qing and L. Zhang, "$(2D)^2$FPCA: An Efficient Approach for Appearance Based Object Recognition", Proceedings of the 3rd International Conference on Bioinformatics and Biomedical Engineering, Beijing, China, **(2009)** June 11-13, pp. 1-4.
[43] J. Yang, J. yu Yang and A. F. Frangi, "Combined Fisher faces Framework", Image Vision Comput., vol. 21, no. 12, **(2003),** pp. 1037-1044.
[44] Z. Wang, Q. Li, X. Niu and C. Busch, "Multimodal Biometric Recognition Based on Complex KFDA", Proceedings of the 5th International Conference on Information Assurance and Security, Xian, China, **(2009)** August 18-20, pp. 177-180.
[45] Information Technology Biometric Performance Testing And Reporting, Part 1: Principles and Framework, ISO/IEC 19795-1, **(2006)**.
[46] S. Wang, Z. Liu, S. Lv, Y. Lv, G. Wu, P. Peng, F. Chen and X. Wang, "A Natural Visible and Infrared Facial Expression Database for Expression Recognition and Emotion Inference", IEEE Trans. Multimedia, vol. 12, no. 7, **(2010)**, pp. 682-691.

## Authors

**Ning Wang** was born in China, in November 1984. He received the B. S degree and M. S. degree in Mathematics in Harbin Institute of Technology (HIT), Harbin, P. R. China in 2006 and 2008, respectively. Now, he is a Ph.D student in the School of Computer Science and Technology, Harbin Institute of Technology. His research interests include iris recognition, face recognition, multi-biometrics recognition, template protection and information theory. E-mail: wangningtop@163.com.

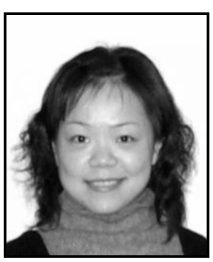

**Qiong Li** was born in China. She received her B.S., M.S. and Ph.D degree from Harbin Institute of Technology, in 1997, 1999 and 2005, respectively. She is now working at Harbin Institute of Technology as an assistant professor. Her research interests include biometric recognition, information security, multimedia security and quantum information security. E-mail: qiongli@hit.edu.cn.

**Ahmed A. Abd El-Latif** was born in Egypt, in July 1984. He received the B.S. degree with honor rank in Mathematics and Computer Science from Menoufia University, Egypt in 2005, and M.S. degree in Computer Science in 2010. He was a teaching assistant in Mathematics department from March 2007 to May 2010. He is currently pursuing the Ph.D. degree at Harbin Institute of Technology (H.I.T), Harbin, P. R. China. He is a referee of many referred international journals and conferences. His areas of interests are cryptography, image segmentation, application of chaotic systems in multimedia content encryption, biometrics encryption, secret image sharing and biometrics. E-mail: ahmed_rahiem@yahoo.com.

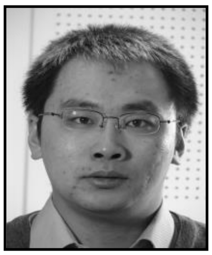

**Jialiang Peng** was born in China, in November 1980. He received the B.S degree and M.S. degree in Computer Science in Heilong Jiang University, Harbin, P. R. China in 2002 and 2005, respectively. Now, he is a Ph.D student in the School of Computer Science and Technology, Harbin Institute of Technology. His research interests include vein recognition, fingerprint recognition, multi-biometrics recognition, template protection and information theory. E-mail: peng80929@163.com.

**Xiamu Niu** was born in China, in May 1961, received the B.S. degree and M.S. degree in Communication and Electronic Engineering from Harbin Institute of Technology (HIT), Harbin, P. R. China in 1982 and 1989 respectively, and received the Ph.D degree in Instrument Science and Technology in 2000. He was an invited scientist and staff member in Department of Security Technology for Graphics and Communication System, Fruanhofer Institute for Computer Graphics, Germany, from 2000 to 2002. He was awarded the Excellent Ph.D Dissertation of China in 2002. He now is the Professor (doctoral advisor) and Superintendent of Information Countermeasure Technique Institute HIT, Director of Information Security Technique Research Center, HIT-ShenZhen. He is SPIE member, ACM member, IEEE member, and the advanced CIE member. He has published 3 works and more than 140 papers cited by SCI and EI. His current research fields include computer information security, hiding communication, cryptography, digital watermarking, signal processing and image processing etc. E-mail: xiamu.niu@hit.edu.cn.